

**THE EFFECT OF PLANTARFLEXION ANGLE ON LANDING MECHANICS
USING A WITHIN-SUBJECTS REAL-TIME FEEDBACK PROTOCOL**

by

K. Michael Rowley

A thesis submitted to the Faculty of the University of Delaware in partial fulfillment of the requirements for the degree of Honors Bachelor of Science in Exercise Science with Distinction

Spring 2013

© 2013 K. Michael Rowley
All Rights Reserved

**THE EFFECT OF PLANTARFLEXION ANGLE ON LANDING MECHANICS
USING A WITHIN-SUBJECTS REAL-TIME FEEDBACK PROTOCOL**

by

K. Michael Rowley

Approved:

James G. Richards, Ph.D.
Professor in charge of thesis on behalf of the Advisory Committee

Approved:

Todd D. Royer, Ph.D.
Committee member from the Department of Kinesiology and Applied
Physiology

Approved:

Victor Kaliakin, Ph.D.
Committee member from the Board of Senior Thesis Readers

Approved:

Michael Arnold, Ph.D.
Director, University Honors Program

ACKNOWLEDGMENTS

I would like to thank Dr. Jim Richards and Dr. Lynnette Overby for being supportive in helping me combine my passions for dance and biomechanics research. I would also like to thank Stephanie Russo, Rob Hulbert, and Kristen Thomas for their assistance in lab and my parents for their constant support.

TABLE OF CONTENTS

LIST OF TABLES	3
LIST OF FIGURES	4
ABSTRACT	6
1 BACKGROUND INFORMATION	7
2 METHODS	10
2.1 Participants	10
2.2 Instrumentation	10
2.3 Experimental Protocol	11
2.4 Statistical Analysis	12
3 RESULTS	14
4 DISCUSSION	22
5 CONCLUSION	27
REFERENCES	28

LIST OF TABLES

Table 1:	Summary of all measurement variables reported using the PF angle heel definition. Means and standard deviation values reported. N values refer to twice the number of landings in each group because each foot was analyzed separately.....	21
Table 2:	Summary of all measurement variables reported using the PF angle ankle joint center definition. Means and standard deviation values reported. N values refer to twice the number of landings in each group because each foot was analyzed separately. This data provided for comparison to previous literature.....	21
Table 3:	Comparison to landing mechanics literature.....	24

LIST OF FIGURES

Figure 1.1: Comparison of two definitions of PF angle. PF angle measurements were taken at initial contact using two definitions of PF angle. There are two data points for each individual landing collected, one for each limb.....	11
Figure 2.1: Screen capture of the real-time feedback program with a photo of the actual foot positions.....	12
Figure 3.1: Peak ground reaction force during weight acceptance for range of plantarflexion angles at landing. Data points are averages of all landings collected between five degrees above and below the plotted point. Error bars show standard deviation. * indicates significant difference at the $p < .05$ level between 0° landings. † indicates significance between 10° landings.	14
Figure 4.1: Peak loading rate between footstrike and peak GRF for range of plantarflexion angles at landing. Data points are averages of all landings collected between five degrees above and below the plotted point. Error bars show standard deviation. * indicates significance difference at the $p < .05$ level between 0° landings. † indicates significance between 10° landings.	15
Figure 5.1: Peak GRF data for subject 19. Data points are averages of all landings collected between five degrees above and below the plotted point. Error bars show standard deviation. Figure 5.2 (Right): Loading rate data for subject 19. Data points are averages of all landings collected between five degrees above and below the plotted point. Error bars show standard deviation. Figure 5.3 (Bottom): Each data point is a measurement taken from one foot during one landing. Filled in circles indicate data from trials where the subject did not receive any instruction for landing.	16
Figure 6.1: Knee sagittal plane angles at landing. Data points are averages of all landings collected between five degrees above and below the plotted point. Error bars show standard deviation. A fully extended knee is 0° and a flexed knee has a negative degree value. Figure 6.2 (Right): Hip sagittal plane angles at landing. A neutral or standing position hip is 0° and a flexed hip has a positive degree value.....	17

Figure 7.1: Knee maximum flexion angles during landing. Data points are averages of all landings collected between five degrees above and below the plotted point. Error bars show standard deviation. More flexion corresponds to a more negative angle. Figure 7.2 (Right): Hip maximum flexion angles during landing. More flexion corresponds to a more positive angle..... 18

Figure 8.1: Peak support moment at each PF angle. Data points are averages of all landings collected between five degrees above and below the plotted point. Error bars show standard deviation..... 19

Figure 9.1: Joint contributions to peak support moment at each PF angle. Data points are averages of all landings collected between five degrees above and below the plotted point. Error bars show standard deviation. For all PF angles, there is a significant difference at the $p < .05$ level between knee and hip contributions. 20

Figure 10.1: Example GRF curves from subject 8. In both figures, the horizontal line represents half body weight. The graph on the left shows a sample GRF curve during a plantarflexed landing. Peak GRF here would be defined as ~800 N. The graph on the right shows a sample GRF curve from a flat-foot landing. Peak GRF here would be defined as ~ 1500 N. 22

ABSTRACT

The mechanics of landing play an important role in the ground reaction forces, joint forces, and joint moments thought to lead to injury in sport. The ankle joint's role in shock absorption has been researched in many studies. Within-subject and between-subjects studies have found that landing with higher amounts of plantarflexion (PF) results in lower peak ground reaction forces (GRFs).^{9,18} There has not yet been a study that compares drop landings within-subjects along a quantitative continuum of PF angles. Subjects were asked to land at a self-selected ankle angle for three trials. Next, using a custom-written real-time feedback program, subjects adjusted their ankles to an instructed angle – between 0° (dorsiflexed) and 50° (plantarflexed) degrees – and dropped onto two force platforms. For increasing PF, peak GRF and peak loading rate decreased significantly. The peak support moment, defined as the sum of the extensor moments in the ankle, knee, and hip²³, also decreased with increasing PF angle. In dorsiflexed landings, the hip and knee were in a more flexed position at landing, and in plantarflexed landings, they were more extended at landing. The hip's contribution to peak total support moment decreased between dorsiflexed landings to 30° plantarflexed landings while the ankle and knee contributions increased between 0° to 30° landings. There appears to be no optimal PF angle to reduce peak GRF and loading rate, but there may be an optimum where joint contributions converge and the hip moment contribution is minimized.

Chapter 1

BACKGROUND INFORMATION

Many research studies have been done on the mechanics of landing in order to identify ways to reduce injury through the reduction of ground reaction forces (GRFs) and joint forces and moments. The lower extremity joints absorb the GRFs upon landing.^{3,6,9,10,13,14,18,20,24,25} Body segment accelerations caused by the GRFs decrease as one travels up the skeleton, leading to the conclusion that forces are dissipating as they pass through the joints.²⁰ Increased GRFs and tibial shock lead to an increased chance of bony injuries such as stress fractures.⁵ An optimal range of lower extremity stiffness appears to protect runners from injury. Studies have found that runners with greater stiffness experience higher incidence of stress fractures than more flexible runners because of the GRFs being absorbed by noncontractile tissues.^{21,22}

In landings from a drop, the stiffness of the lower extremity is mainly controlled by the ankle.² As the landing height and velocity increase, people naturally extend the knee and ankle joints more at initial landing as well as increase the total joint range of motion during the absorption phase of landing.^{14,19,24} Regardless of drop height and velocity, the peak ground reaction force can be reduced when subjects are instructed to land with increased PF.^{4,13,18} Kovacs et. al. found that ground reaction forces were significantly higher in heel-toe landings than forefoot landings within subjects.⁹ They calculated that the ankle plantarflexors dissipated the most energy in the forefoot landing, but were second to the knee and hip extensors in the heel-toe landing. They also speculate that in the heel-toe landing, a greater amount of energy is

dissipated into the noncontractile tissues (bones, cartilage, ligaments, etc), in contrast to forefoot landings where most of the absorption happened in the musculature.⁹ Self and Paine instructed subjects to land one of four qualitative ways: natural landing, stick the landing, stick the landing and flex your calf muscles, and stick the landing but land more flat-footed.¹⁸ The last condition showed the highest peak vertical forces and highest tibial accelerations.¹⁸ In a study done by Fugii et. al., subjects instructed to land “with full PF” or “like a ballet dancer” could reduce the peak GRF during landing compared to an uninstructed landing.⁴

Information about landing mechanics and plantarflexion angle has specific applications in ice skating and in dance. Ice skaters must always land with stiff dorsiflexion because of the constraints of their boots. They have high incidents, up to 20%, of stress fractures.^{1,16} There is an increasing number of lumbar spine stress fractures thought to be a result of hip flexion and lumbar extension at landing because of a limitation in ankle PF and knee flexion caused by the skating boot.¹¹ Dancers, who always land with extreme PF, experience similar landing GRFs^{10,17} but have a very low incidence of stress fractures.^{7,8}

All studies have found that groups with higher amounts of PF have lower peak GRFs. No study has yet compared drop landings within subjects along a continuum of quantitative PF angles using real-time feedback motion analysis software. Knowing how GRF is affected along a continuum of PF angles will inform future studies on sport landing training, ice skating boot design, and dance injury research.

It was predicted that at a PF angle between 20° and 30°, peak GRF and/or peak loading rate during weight acceptance would be minimized. The muscle length-tension curve suggests that there may be an optimal ankle orientation at which the

gastrocnemius and soleus are near resting length and are able to produce the greatest tension, maximizing heel deceleration between initial contact and weight acceptance. In addition, it was predicted that the ankle orientation of the uninstructed landings would be near that minimum as the body naturally attempts to minimize these forces traveling up the lower extremities.

Chapter 2

METHODS

2.1 Participants

Twenty-five subjects were recruited, 17 females and 8 males. Age was 21.4 ± 2 years. Dancers were actively recruited because of their greater PF range of motion. Twelve of the subjects had been training in dance for at least five years. IRB procedures were followed in subject recruitment and testing.

2.2 Instrumentation

Three-dimensional lower extremity kinematic data were collected using a seven-camera motion capture system at a sampling rate of 120 Hz (Motion Analysis Corporation, Santa Rosa, CA). Retroreflective markers were placed on the lower limbs using a modified Helen Hayes marker set. Kinetics were collected using two AMTI forceplates sampled at 1200 Hz (Advanced Medical Technology Inc., Model OR6). Each forceplate was covered with a 1.2cm-thick foam pad.

PF angles were defined as the angle between a vector drawn from the ankle joint center to the knee joint center and a vector drawn from the heel marker to the toe marker. The ankle is at 0° PF when in a standing, neutral position. Previous literature has defined PF angle as the angle between a vector from the ankle joint center to the knee joint center and a vector from the ankle joint center to the toe marker. Measurements of PF angle at initial contact using these two definitions are highly correlated at $R = .9889$ (Figure 1.1). Experimental results using the second definition

are summarized in Table 2 for ease of comparison to previous literature. Conversions between PF angle measurements reported in this study and those in literature can also be estimated using the equation given in Figure 1.1.

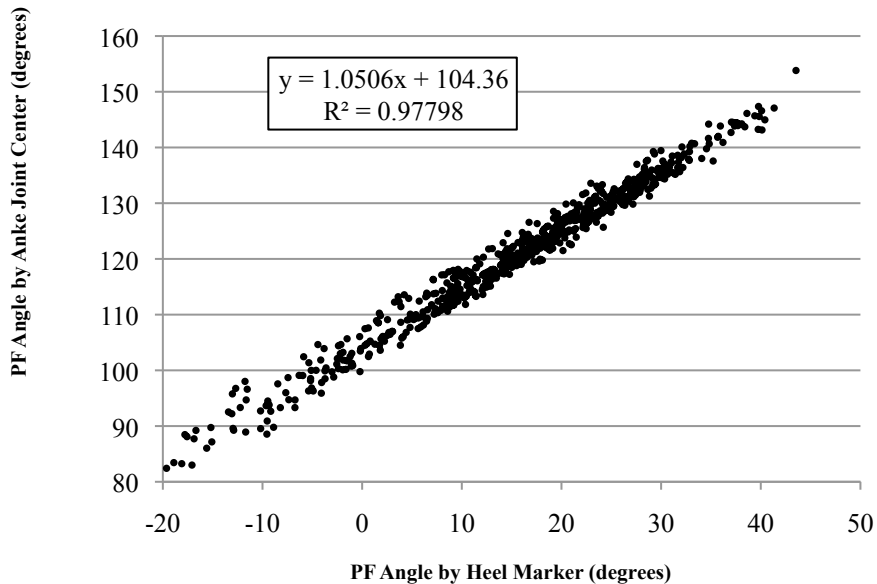


Figure 1.1: Comparison of two definitions of PF angle. PF angle measurements were taken at initial contact using two definitions of PF angle. There are two data points for each individual landing collected, one for each limb.

2.3 Experimental Protocol

Subjects were fitted with the retroreflective markers, a static collection was taken, and a range of motion trial was taken to calculate functional hip joint centers using a sphere fitting algorithm. Subjects then held themselves from a bar suspended at their maximum vertical jump height. They were allowed to drop onto two AMTI forceplates until they felt comfortable doing so barefoot. Three drops were collected where the subjects could see a projection of their ankle angles, but did not receive any instruction for how to position them. For data analysis these were termed uninstructed

landings. Then the subjects were asked to position their ankles at either 0° (flat-foot), 10°, 20°, 30°, 40°, and 50° (full PF) using the real-time feedback program pictured in Figure 2.1. Order was randomized. They were asked to drop onto the forceplates holding the desired ankle position until contact, and then to absorb the fall however they felt necessary. They were also instructed to keep their arms above their head throughout the drop and landing. A maximum of five trials were captured for each target ankle angle or until the subject achieved the landing within ten degrees of the target. Not all subjects could achieve landings at 40° and 50° PF.

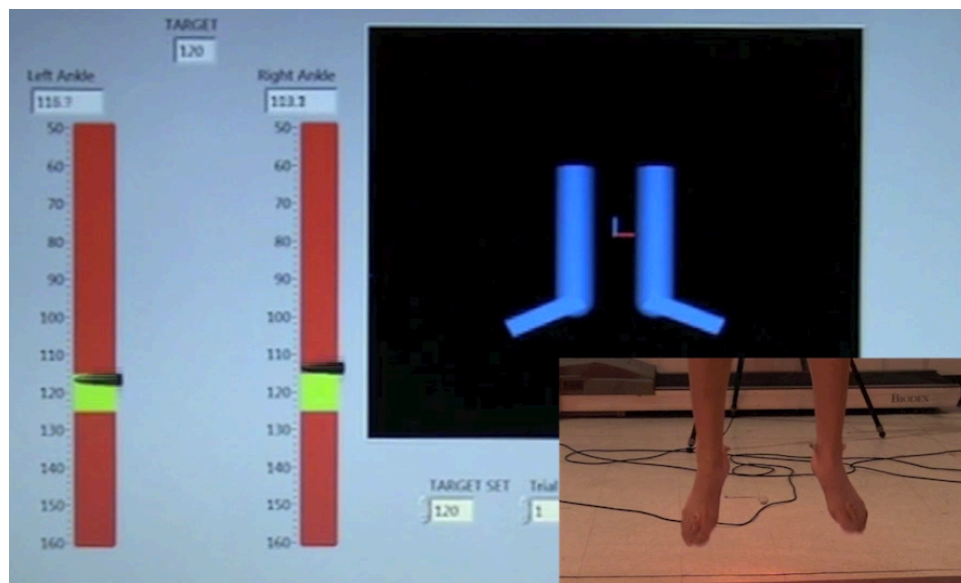


Figure 2.1: Screen capture of the real-time feedback program with a photo of the actual foot positions.

2.4 Statistical Analysis

Measurement variables included peak GRF in times body weight (xbw) during weight acceptance, peak loading rate as defined by the maximum derivative of the vertical GRF curve leading up to the peak GRF at weight acceptance, knee and hip

sagittal angles at initial contact, maximum flexion of the knee and hip, and lower extremity joint contributions to the peak support moment during the landing. Weight acceptance was defined as the portion of the GRF curve from just after initial contact (toe-strike) to the next peak in GRF. While all data points are reported in the results section, only 11 subjects successfully completed landings in all categories 0°-40°. Only these eleven subjects were used for the Tukey Post-Hoc analysis.

Chapter 3

RESULTS

The mean ankle angle at initial contact for uninstructed landings was $17.19^\circ \pm 6.8^\circ$ PF. Peak GRF during weight acceptance decreased from 3.13 times body weight (xbw) when landing flat-footed (0° PF) to 1.49 xbw at 40° PF (Figure 3.1). Peak loading rate between footstrike and peak GRF also decreased. The maximum of the derivative of the GRF curve of landings at 0° PF averaged 315.31 body weights per second (bw/s). This decreased to 42.04 bw/s in landings at 40° PF (Figure 4.1).

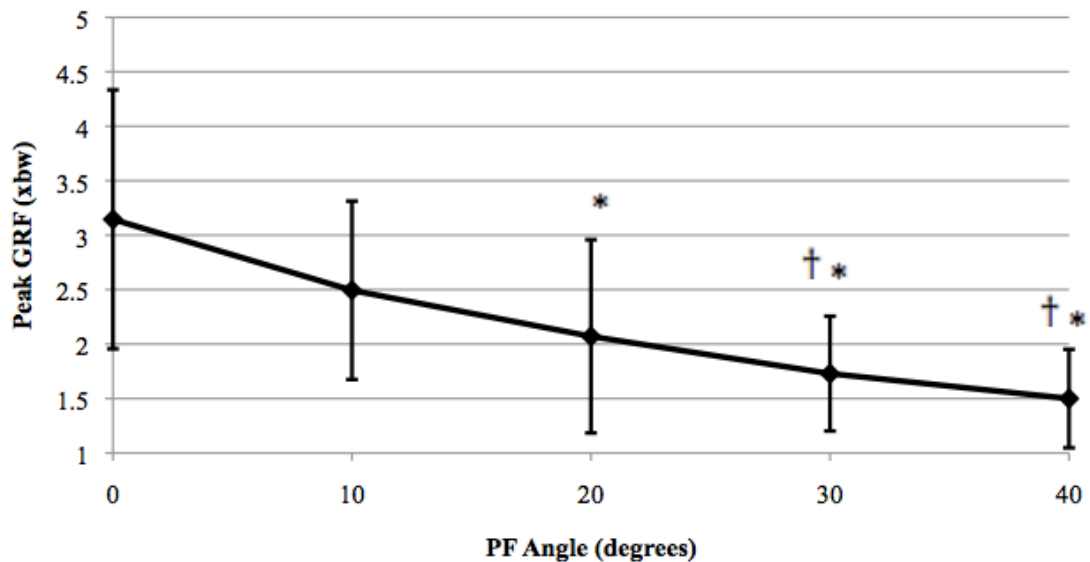


Figure 3.1: Peak ground reaction force during weight acceptance for range of plantarflexion angles at landing. Data points are averages of all landings collected between five degrees above and below the plotted point. Error bars show standard deviation. * indicates significant difference at the $p < .05$ level between 0° landings. † indicates significance between 10° landings.

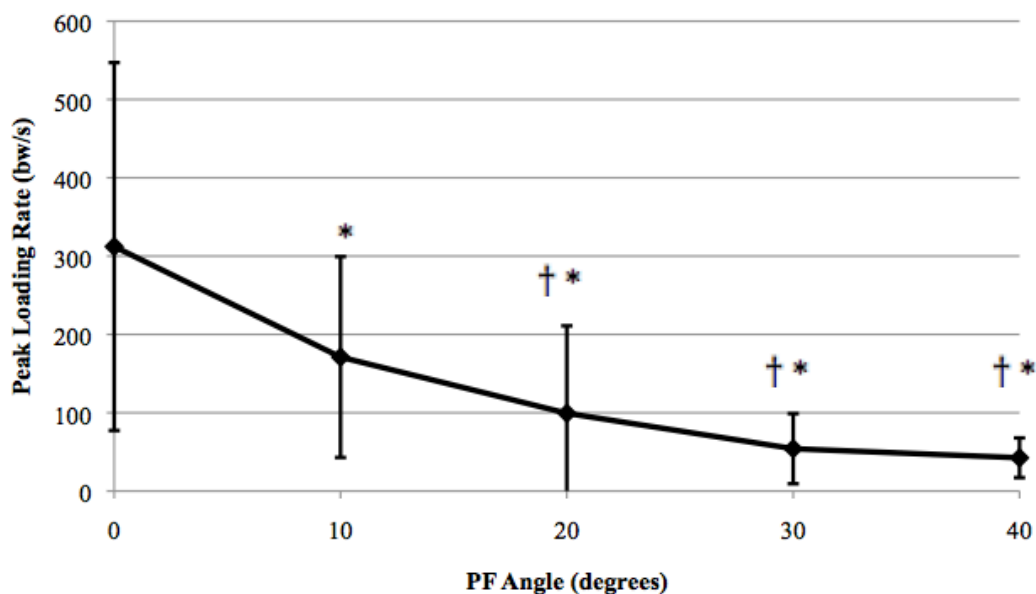


Figure 4.1: Peak loading rate between footstrike and peak GRF for range of plantarflexion angles at landing. Data points are averages of all landings collected between five degrees above and below the plotted point. Error bars show standard deviation. * indicates significance difference at the $p < .05$ level between 0° landings. † indicates significance between 10° landings.

In some subjects there were clear minima reached for either the peak GRF measurement, the peak loading rate measurement or both. Six subjects showed a minimization of one or both of these measurements at landing PF angles of 20° or 30° . Figures 5.1 and 5.2 show the GRF and the loading rate graphs for subject 19, one of the subjects who showed a minimization. A distinct minimum for the peak GRF at the 20° PF landings is visible. There is a less distinct minimum in the peak loading rate for these landings as well. Figure 5.3 shows the raw peak GRF data for subject 19. The cluster of data points representing uninstructed landings appears at PF angles slightly greater than where peak GRF is minimized. Not all subjects' data revealed a minimum for either of these variables.

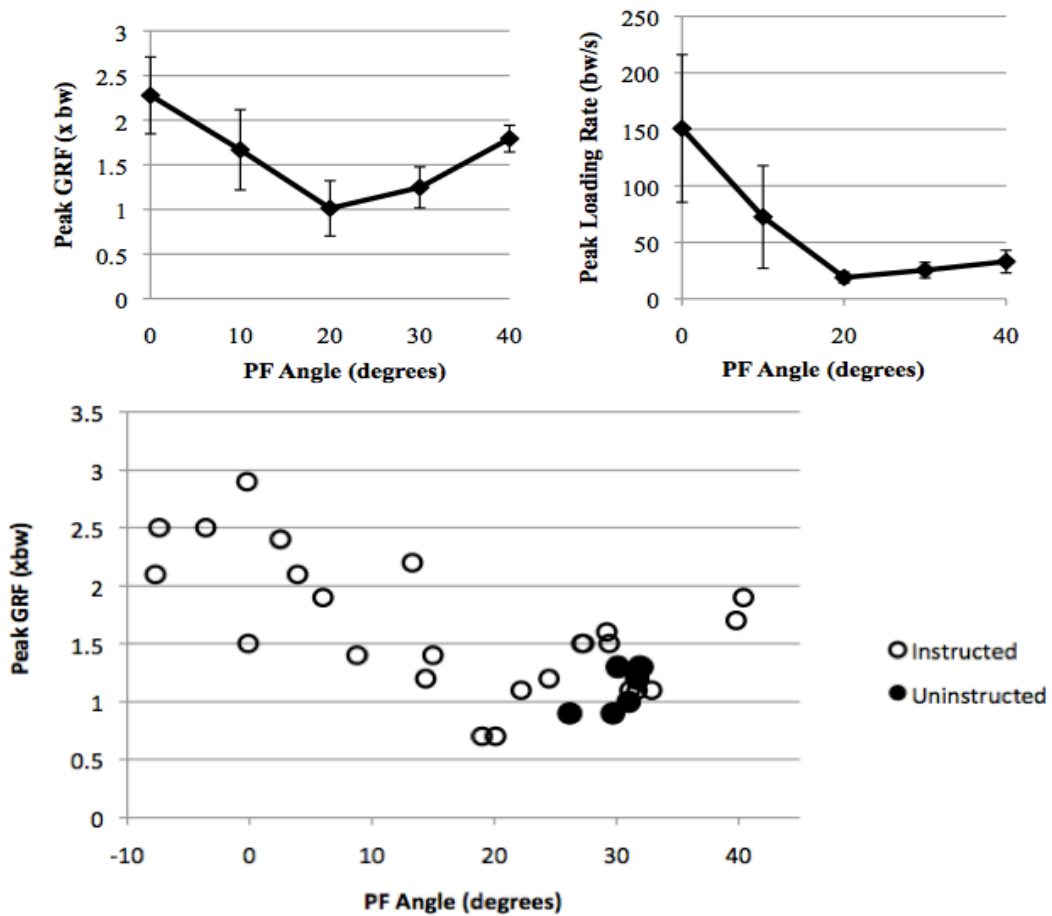


Figure 5.1 (Left): Peak GRF data for subject 19. Data points are averages of all landings collected between five degrees above and below the plotted point. Error bars show standard deviation.

Figure 5.2 (Right): Loading rate data for subject 19. Data points are averages of all landings collected between five degrees above and below the plotted point. Error bars show standard deviation.

Figure 5.3 (Bottom): Each data point is a measurement taken from one foot during one landing. Filled in circles indicate data from trials where the subject did not receive any instruction for landing.

Measurements of knee and hip sagittal plane kinematics as an effect of PF angle at landing indicate that both joints trend toward increased extension at landing as PF increases (Figures 6.1 and 6.2). There was a small decrease in the maximum flexion reached by the knee and hip during landing as PF increased (Figures 7.1 and 7.2).

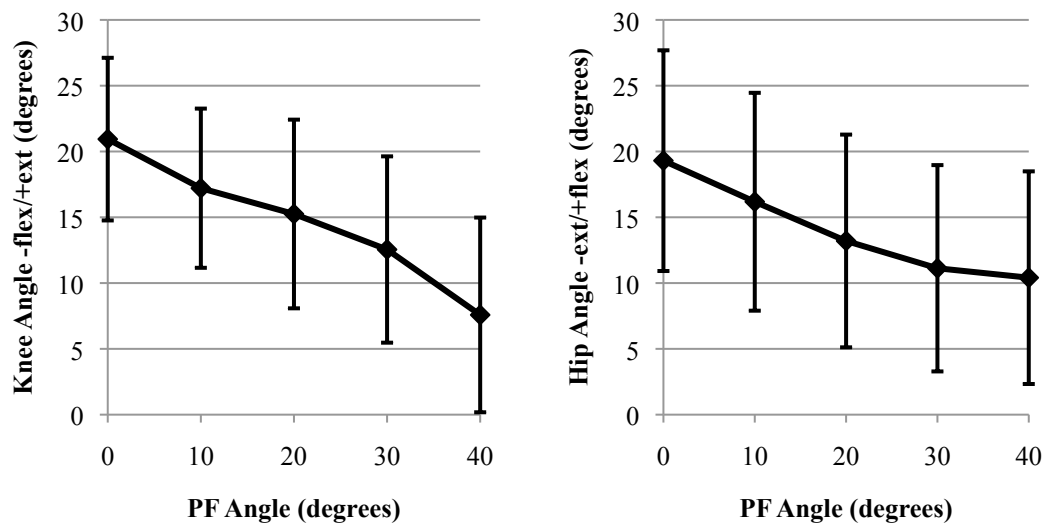


Figure 6.1 (Left): Knee sagittal plane angles at landing. Data points are averages of all landings collected between five degrees above and below the plotted point. Error bars show standard deviation. A fully extended knee is 0° and a flexed knee has a negative degree value.

Figure 6.2 (Right): Hip sagittal plane angles at landing. A neutral or standing position hip is 0° and a flexed hip has a positive degree value.

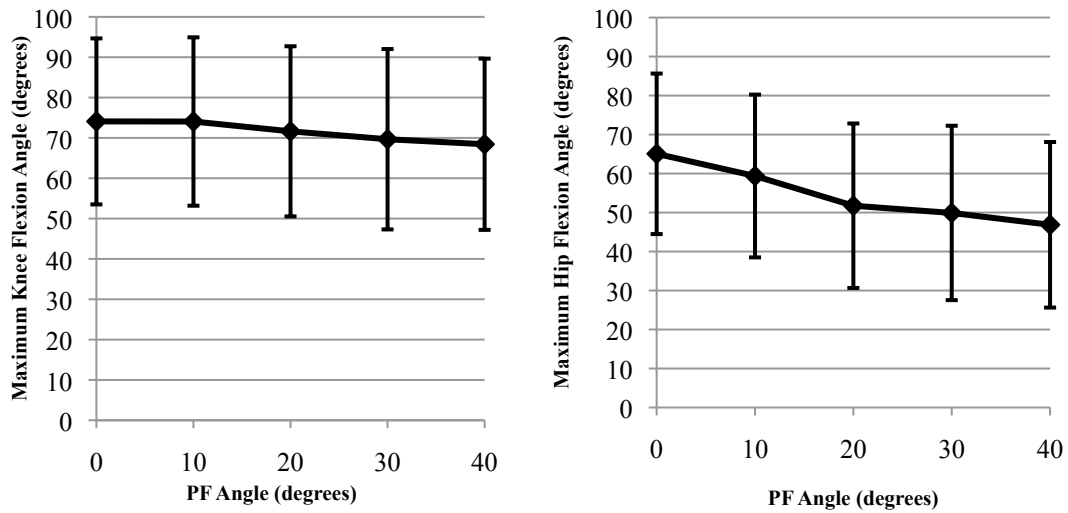


Figure 7.1 (Left): Knee maximum flexion angles during landing. Data points are averages of all landings collected between five degrees above and below the plotted point. Error bars show standard deviation. More flexion corresponds to a more negative angle.

Figure 7.2 (Right): Hip maximum flexion angles during landing. More flexion corresponds to a more positive angle.

Peak support moment during landing was calculated as the sum of the extensor moments of each lower extremity joint.²³ The trend is similar to the peak GRF trend decreasing from 5.02 Nm/bw at 0° landings to 2.68 Nm/bw at 40° landings (Figure 8.1). A joint contribution value was calculated for each joint by dividing the sagittal moment of that joint at the same instant of the peak support moment by the value of the peak support moment. These are reported as percentages in Figure 9.1. The contribution of hip moment decreased from 75.2% ± 17% at 0° PF landings to 35.3% ± 21% at 30° PF landings. The contribution then increased again at 40° PF landings. The ankle and knee contributions increased from 0° PF landings to 30° PF landings

then decreased at 40° PF landings. There appeared to be a convergence of these three variables at 30° PF landings.

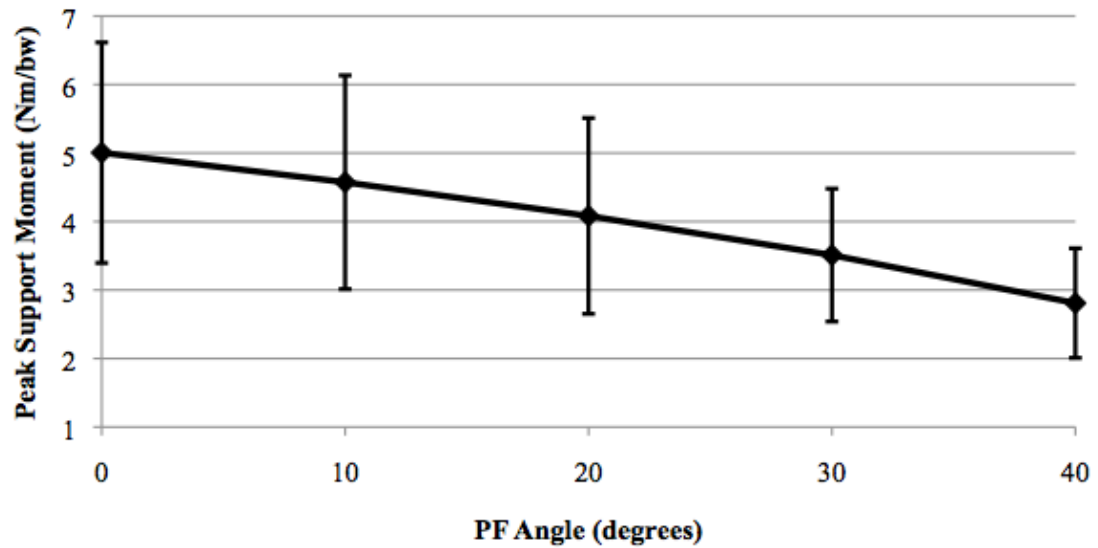


Figure 8.1: Peak support moment at each PF angle. Data points are averages of all landings collected between five degrees above and below the plotted point. Error bars show standard deviation.

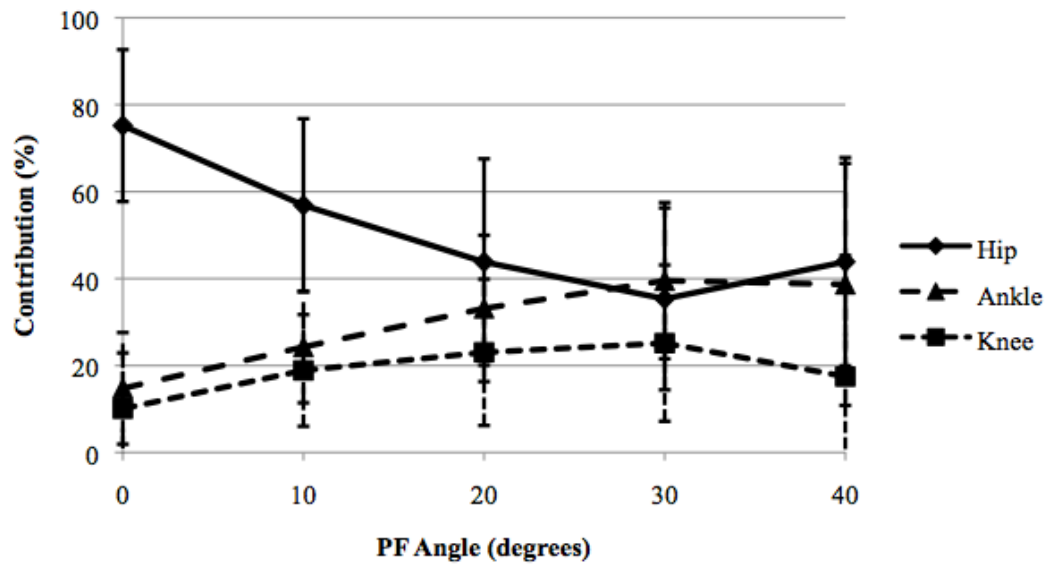


Figure 9.1: Joint contributions to peak support moment at each PF angle. Data points are averages of all landings collected between five degrees above and below the plotted point. Error bars show standard deviation. For all PF angles, there is a significant difference at the $p < .05$ level between knee and hip contributions.

Table 1: Summary of all measurement variables reported using the PF angle heel definition. Means and standard deviation values reported. N values refer to twice the number of landings in each group because each foot was analyzed separately.

PF Angle	0° N=95		10° N=157		20° N=205		30° N=108		40° N=25	
	Mean	SD	Mean	SD	Mean	SD	Mean	SD	Mean	SD
Peak GRF (x bw)	3.15	1.19	2.49	0.82	2.07	0.89	1.73	0.53	1.50	0.45
Peak Loading Rate (bw/s)	312.15	234.92	171.07	128.27	99.28	111.71	54.06	44.77	42.45	25.37
Knee Angle at Landing (deg)	20.94	6.18	17.21	6.05	15.25	7.17	12.55	7.08	7.58	7.40
Hip Angle at Landing (deg)	19.03	8.39	16.18	8.28	13.20	8.08	11.13	7.84	10.41	8.08
Peak Support Moment (Ms) (Nm/bw)	5.01	1.61	4.57	1.56	4.08	1.43	3.51	1.19	2.81	0.87
Ankle Contribution to Ms (%)	14.75	9.61	24.27	11.55	31.14	12.68	39.52	12.70	38.66	11.93
Knee Contribution to Ms (%)	10.07	12.84	18.87	12.85	20.03	16.83	25.15	17.97	17.47	27.84
Hip Contribution to Ms (%)	75.19	17.47	56.86	19.91	43.82	23.73	35.33	20.93	43.87	23.95

Table 2: Summary of all measurement variables reported using the PF angle ankle joint center definition. Means and standard deviation values reported. N values refer to twice the number of landings in each group because each foot was analyzed separately. This data provided for comparison to previous literature.

PF Angle	105° N=90		115° N=155		125° N=189		135° N=118		145° N=30	
	Mean	SD	Mean	SD	Mean	SD	Mean	SD	Mean	SD
Peak GRF (x bw)	3.19	1.32	2.47	0.80	2.13	0.95	1.76	0.56	1.52	0.43
Peak Loading Rate (bw/s)	323.59	275.83	164.04	123.69	108.41	123.81	57.82	52.32	43.94	25.53
Knee Angle at Landing (deg)	21.00	6.02	16.89	5.81	14.89	7.00	13.29	7.43	8.50	7.60
Hip Angle at Landing (deg)	19.57	7.95	16.05	7.85	13.27	8.17	10.71	7.90	10.98	7.96
Peak Support Moment (Ms) (Nm/bw)	5.09	1.65	4.53	1.55	4.13	1.47	3.58	0.97	2.86	0.74
Ankle Contribution to Ms (%)	15.28	9.71	24.68	11.56	32.54	12.87	39.19	12.75	37.62	12.17
Knee Contribution to Ms (%)	10.27	13.93	18.27	12.95	23.07	15.98	24.89	17.59	20.80	27.62
Hip Contribution to Ms (%)	74.45	19.26	57.05	20.22	44.39	23.24	35.92	21.56	41.57	23.26

Chapter 4

DISCUSSION

As previous studies have shown, flat-foot landings produce a GRF curve with a large initial peak while plantarflexed landings produce a GRF curve with two smaller peaks, one at toe-strike and one at weight acceptance.¹⁵ For this study, peak GRF measurements were taken from the peak after toe-strike or from the initial peak in cases where there is only one large peak. Figure 10.1 shows example GRF curves from subject 8.

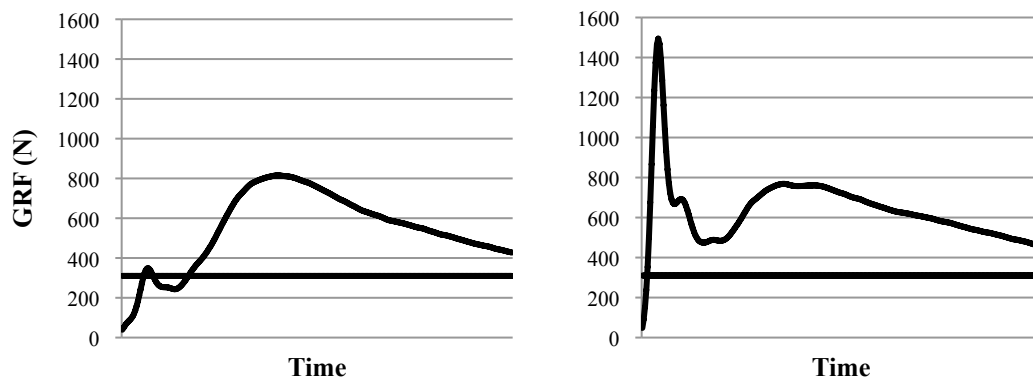


Figure 10.1: Example GRF curves from subject 8. In both figures, the horizontal line represents half body weight. The graph on the left shows a sample GRF curve during a plantarflexed landing. Peak GRF here would be defined as ~800 N. The graph on the right shows a sample GRF curve from a flat-foot landing. Peak GRF here would be defined as ~ 1500 N.

As PF angle at landing increases from flat-footed (0° PF) to 20° PF, the peak GRF and peak loading rates decrease significantly. PF greater than 20° did not produce significant decreases in GRF, although GRF trended lower at 30° and 40° PF. While the prediction of a minimization in peak GRF and/or peak loading rate at some optimal ankle orientation was observed in some subjects, it was not inclusive. Only 6 of 25 subjects showed a minimum in one or both of these measurement variables. In addition, of the six subjects showing a minimization of peak GRF or peak loading rate, none had uninstructed landings with PF angles at these minima as was predicted.

The group's uninstructed landings were $17.19^\circ \pm 6.8^\circ$ PF. It is important to note that an uninstructed PF angle of 17.19° is unique to the testing conditions, which included barefoot landings and foam pads over each force plate. Removing the pads and asking subjects to wear sneakers would likely result in a change in uninstructed PF angle. When PF angle is calculated using the ankle joint center, as described in the methods section, uninstructed landings had an ankle angle of $122.49^\circ \pm 7.2^\circ$ PF. This is comparable to previous literature which cites natural barefoot landings onto a similar padded forceplate at $125.7^\circ \pm 6.4^\circ$ PF.¹⁸ The peak GRF measurement for the uninstructed landings in this study was 2.39 ± 0.92 xbw, which when doubled to 4.70 xbw to account for both legs, also compares favorably to the Self and Paine's results of 4.29 xbw.¹⁸ The peak GRF of 3.15 xbw for 0° landings when doubled to 6.30 xbw compares favorably to other studies measuring "stiff knee" and "flatfoot" landings with GRFs between 6.18 and 6.74 xbw.^{15,18} Ground reaction force data from this study compares favorably to previous literature, which is summarized in Table 3.

Table 3: Comparison to landing mechanics literature.

Study	Landing Style	Peak GRF (xbw)
Rowley, Richards (current study): From maximum vertical jump height. Quantitative PF angle displayed real-time for matching. Values doubled for comparison.	40° PF	3.00
	30° PF	3.46
	20° PF	4.14
	10° PF	4.98
	0° PF	6.29
Self, Paine (2001) ¹⁸ : From .305m. Qualitative landing descriptions. Values doubled for comparison.	Bent Knee	4.29
	Stiff Knee	5.84
	Stiff-Kneed, Max PF	4.11
	Stiff-Kneed, Land on Heels	6.74
Zhang, Dufek, Bates (2000) ²⁶ : Values averaged from drops at 0.32 m, 0.62m, and 1.03 m and doubled for comparison. Qualitative instructions.	Soft	5.95
	Normal	6.73
	Stiff	8.46
Mizrahi, Susak (1982) ¹⁵ : From 0.5m onto one foot only.	Flat-foot	6.18

All lower extremity joints play a large role in attenuating GRF at landing due to the activity of biarticular muscles. In this study, PF angle was controlled while knee and hip motion were unconstrained. Both hip and knee joints showed more extension at initial contact as PF angle increased. This agrees with previous literature, which identifies the ankle as the main determining factor in lower extremity joint stiffness in hopping.² There was a slight decrease in the maximum flexion angle reached for both the hip and knee as PF angle increased. We theorize that less motion at these joints was required to attenuate the landing forces when increased motion at the ankle was allowed.

All three joints play a role in support during a drop. The sum of the extensor moments in the three joints is defined as the support moment.²³ Graphing the peak support moment during landing against PF angle reveals a trend similar to that of the peak GRF. Peak support moment decreases as PF angle increases with no clear minimum. The roles of each joint were quantified as a percent of the peak support

moment during the landing. In landings at 0° PF, the hip contributed $75.2\% \pm 17\%$ of the peak support moment, which was also highest during landings in this position. These large joint moments calculated from GRF and center of pressure measurements correspond to even larger joint contact forces, because there is an underestimation due to the inability to measure force applied by musculature. Therefore, it is suspected that hip contact forces were very high in landings with this ankle orientation.

As PF angle increased, both the ankle and knee contributions increased while the hip contribution decreased. At 30° PF the hip, knee, and ankle contributions were 35%, 25%, and 40% respectively. This is the only landing condition in which the ankle's contribution to the peak support moment was larger than the hip's contribution. Previous investigations that have allowed subjects to choose their ankle orientation at landing have found that the ankle is the primary mechanism for regulating lower extremity stiffness and for absorbing GRF.^{2,9} While this may be true for uninstructed landings near 20° or 30° PF, the results of this study show it is not true for instructed landings with less PF. A possible optimal ankle orientation to protect all three joints may be at 30° PF because, beyond this angle, the contribution of the hip moment begins to increase again from 35% to 44%.

In the context of certain activities, these data's importance becomes apparent. Figure skaters represent a unique sport population since ankle motion is constrained in a boot during landings. There is anecdotal evidence of a high incidence hip injury in elite figure skaters. Two of the most publicized hip injuries were Rudy Gilando's double hip replacements at age 34 and Tara Lipinski's, the youngest individual gold medalist in the history of the Olympic Winter Games, hip surgery at age 18. It is suspected this is because figure skaters repeatedly land at close to 0° PF, and hip

moments contribute approximately 75% of the total peak support moment. There are also data to suggest that this high hip moment is achieved by lumbar extension and is a leading cause of lumbar spine stress fractures in figure skaters as well.¹¹ This study suggests that freeing the ankle to plantarflex at landing can potentially reduce the high hip moments and decrease the incidence of hip injury and lumbar spine stress fractures.

The biggest limitation of this study was the inability for all subjects to achieve landings in each category of PF. Categories tested were 0°, 10°, 20°, 30°, 40°, and 50° PF. Landings at 50° were not analyzed because there were too few subjects who completed this condition. There were only 11 subjects who achieved landings in all categories between 0°-40°. It appeared some subjects did not have active range of motion to reach PF angles larger than 30°. Other subjects could reach these angles while suspended but could not maintain them during the drop and therefore landed slightly less plantarflexed.

Future studies should investigate how uninstructed PF angle changes after multiple drops. It is predicted that as a result of fatigue, the PF angle will increase in order to decrease the GRF after many repeated drops. Changing landing conditions such as adding sneakers or removing the foam pads would also change uninstructed PF angle. A similar protocol could use the real-time feedback program to control knee or hip angle at landing and measure motion of the other two joints as dependent variables. Analysis could be expanded to the upper body in order to evaluate lumbar spine motion. This would provide the connection between high hip moments and increased lumbar spine extension.

Chapter 5

CONCLUSION

As PF angle at initial contact increases, peak GRF, peak loading rate, and peak support moment decrease. There is no clear minimization in most subjects through the range of PF tested. Even for subjects that do show a minimization, the uninstructed landings do not fall in this range. This study contributes two novel pieces of information to the literature. First, by plantarflexing more than the natural ankle angle at landing, peak GRFs can be reduced. Second, there is a high contribution from the hip to the peak total support moment during landings with little to no PF. This high contribution could be indicative of high risk to the hip joint in certain sport-specific landing activities such as figure skating.

REFERENCES

1. Dubravcic-Simunjak. (2003). The incidence of injuries in elite junior figure skaters. *The American Journal of Sports Medicine* , 31 (4), 511-17.
2. Farley, C. T., & Morgenroth, D. C. (1999). Leg stiffness primarily depends on ankle stiffness during human hopping. *Journal of Biomechanics* , 32, 267-73.
3. Fong, C. M., Blackburn, J. T., Norcross, M. F., McGrath, M., & Padua, D. A. (2011). Ankle-dorsiflexion range of motion and landing biomechanics. *J Athl Train* , 46 (1), 5-10.
4. Fugii, E., Urabe, Y., Yamanaka, Y., Shinohara, H., Sasadai, J., Takai, S., et al. (2011). The effect of ballet landing technique on ground reaction force and muscle activation. In R. Solomon, & J. Solomon (Ed.), *International Association for Dance Medicine and Science 21st Annual Meeting*, (pp. 99-100). Washington, D.C.
5. Grimston, S. K., Ensberg, J. R., Kloiber, R., & Hanley, D. A. (1991). Bone mass, external loads, and stress fractures in female runners. *Journal of Applied Biomechanics* , 7 (3), 293-302.
6. Gross, T. S., & Nelson, R. C. (1988). The shock attenuation role of the ankle during landing from a vertical jump. *Med Sci Sports Exerc* , 20 (5), 506-14.
7. Hardaker, W. T. (1989). Foot and ankle injuries in classical ballet dancers. *The Orthopedic Clinics of North America* , 20 (4), 621-27.
8. Harrington, T., Crichton, K. C., & Anderson, I. F. (1993). Overuse ballet injury of the base of the second metatarsal. *American Journal of Sports Medicine* , 21, 591-98.
9. Kovacs, I., Tihanvi, J., Devita, P., Racz, L., Barrier, J., & Hortobagvi, T. (1999). Foot placement modifies kinematics and kinetics during drop jumping. *Med Sci Sports Exerc* , 31 (5), 708-16.

10. Kulig, K., Fietzer, A. L., & Popovich, J. M. (2011). Ground reaction forces and knee mechanics in the weight acceptance phase of a dance leap take-off and landing. *J Sports Sci* , 29 (2), 125-31.
11. Lipetz, J., & Kruse, R. J. (2000). Injuries and special concerns of female figure skaters. *Clinics in sports medicine* , 12 (2), 369-80.
12. Mache, M. A., Hoffman, M. A., Hannigan, K., Golden, G. M., & Pavol, M. J. (2012). Effects of decision making on landing mechanics as a function of task and sex. *Clinical Biomechanics* , In print.
13. McNair, P. J., Prapavessis, H., & Callender, K. (2000). Decreasing landing forces: effects of instruction. *Br J Sports Med* , 34, 293-96.
14. McNitt-Gray, J. L. (1993). Kinetics of the lower extremities during drop landings from three heights. *J Biomech* , 26 (9), 1037-46.
15. Mizrahi, J., & Susak, Z. (1982). Analysis of parameters affecting impact force attenuation during landing in human vertical free fall. *Engineering in Medicine* , 11, 141.
16. Pecina, M., Bojanic, I., & Dubravcic, S. (1990). Stress fractures in figure skaters. *The American Journal of Sports Medicine* , 18, 277-79.
17. Richards, J. G., & Bruening, D. A. (2006). The effects of articulated figure skates on jump landing forces. *J Appl Biomech* , 22 (4), 285-95.
18. Self, B. P., & Paine, D. (2001). Ankle biomechanics during four landing techniques. *Med Sci Sports Exerc* , 33 (8), 1338-44.
19. Whitting, J. W., Steele, J. R., Jaffrey, M. A., & Munro, B. J. (2007). Parachute landing fall characteristics at three realistic vertical descent velocities. *Aviat Space Environ Med* , 78 (12), 1135-42.
20. Whitting, J. W., Steele, J. R., McGhee, D. E., & Munro, B. J. (2011). Dorsiflexion capacity affects achilles tendon loading during drop landings. *Med Sci Sports Exerc* , 43 (4), 706-13.
21. Williams, D. S., Davis, I. M., Scholz, J. P., Hamill, J., & Buchanan, T. S. (2004). High-arched runners exhibit increased leg stiffness compared to low-arched runners. *Gait and Posture* , 19, 263-69.
22. Williams, D. S., McClay, I. S., & Hamill, J. (2001). Arch structure and injury patterns in runners. *Clinical Biomechanics* , 16, 341-47.

23. Winter, D. A. (1980) Overall principle of lower limb support during stance phase of gait. *J Biomechanics* , 13, 923-7.
24. Yeow, C. H., Lee, P. V., & Goh, J. C. (2009). Regression relationships of landing height with ground reaction forces, knee flexion angles, angular velocities and joint powers during double-leg landing. *Knee* , 16 (5), 381-86.
25. Yu, B., Lin, C. F., & Garrett, W. E. (2006). Lower extremity biomechanics during the landing of a stop-jump task. *Clin Biomech (Bristol, Avon)* , 21 (3), 297-305.
26. Zhang, S., Bates, B. T., & Dufek, J.S. (1998) Contributions of lower extremity joints to energy dissipation during landings. *Med Sci Sports xExerc* , 32 (4), 812-9.